Differentiable Task Graph Learning: Procedural Activity Representation and Online Mistake Detection from Egocentric Videos

Luigi Seminara Giovanni Maria Farinella Antonino Furnari

Department of Computer Science, University of Catania luigi.seminara@phd.unict.it,{giovanni.farinella,antonino.furnari}@unict.it

Abstract

Procedural activities are sequences of key-steps aimed at achieving specific goals. They are crucial to build intelligent agents able to assist users effectively. In this context, task graphs have emerged as a human-understandable representation of procedural activities, encoding a partial ordering over the key-steps. While previous works generally relied on hand-crafted procedures to extract task graphs from videos, in this paper, we propose an approach based on direct maximum likelihood optimization of edges' weights, which allows gradient-based learning of task graphs and can be naturally plugged into neural network architectures. Experiments on the CaptainCook4D dataset demonstrate the ability of our approach to predict accurate task graphs from the observation of action sequences, with an improvement of +16.7% over previous approaches. Owing to the differentiability of the proposed framework, we also introduce a feature-based approach, aiming to predict task graphs from key-step textual or video embeddings, for which we observe emerging video understanding abilities. Task graphs learned with our approach are also shown to significantly enhance online mistake detection in procedural egocentric videos, achieving notable gains of +19.8% and +7.5% on the Assembly 101 and EPIC-Tent datasets. Code for replicating experiments is available at https:// github.com/fpv-iplab/Differentiable-Task-Graph-Learning.

1 Introduction

Procedural activities are fundamental for humans to organize tasks, improve efficiency, and ensuring consistency in the desired outcomes, but require time and effort to be learned and achieved effectively. This makes the design of artificial intelligent agents able to assist users to correctly perform a task appealing [19, 27]. Achieving these abilities requires building a flexible representation of a procedure, encapsulating knowledge on the partial ordering of key-steps arising from the specific context at hand. For example, a virtual assistant needs to understand that it is necessary to break eggs before mixing them or that the bike's brakes need to be released before removing the wheel. Importantly, for a system to be scalable, this representation should be automatically learned from observations (e.g., humans making a recipe many times) rather than explicitly programmed by an expert.

Previous approaches focused on directly tackling tasks requiring procedural knowledge such as action anticipation [15, 13, 30] and mistake detection [33, 12, 6, 37, 14] without developing explicit representations of the procedure. Other works proposed neural models able to develop implicit representations of the procedure by learning how to recover missing actions [39, 25], discover keysteps [10, 4, 5], or grounding them to video [9, 22]. A different approach [3, 9, 16] consists in representing the structure of a procedure in the form of a *task graph*, i.e., a Directed Acyclic Graph (DAG) in which nodes represent key-steps, and directed edges impose a partial ordering over key-steps,

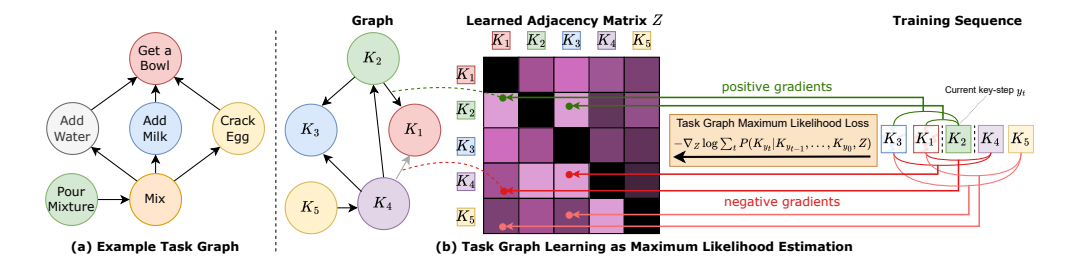


Figure 1: (a) An example task graph encoding dependencies in a "mix eggs" procedure. (b) We learn a task graph which encodes a partial ordering between actions (left), represented as an adjacency matrix Z (center), from input action sequences (right). The proposed Task Graph Maximum Likelihood (TGML) loss directly supervises the entries of the adjacency matrix Z generating gradients to maximize the probability of edges from past nodes (K_3, K_1) to the current node (K_2) , while minimizing the probability of edges from past nodes to future nodes (K_4, K_5) in a contrastive manner.

encoding dependencies between them (see Figure 1(a)). Graphs provide an explicit representation which is readily interpretable by humans and easy to incorporate in downstream tasks such as detecting mistakes or validating the execution of a procedure. While graphs have been historically used to represent constraints in complex tasks and design optimal sub-tasks scheduling [34], graph-based representations mined from videos [3], key-step sequences [35, 18] or external knowledge bases [40] have only recently emerged as a powerful representation of procedural activities able to support downstream tasks such as key-step recognition or forecasting [3, 40]. Despite these efforts, current methods rely on meticulously crafted graph mining procedures rather than setting graph generation in a learning framework, limiting the inclusion of task graph representations in end-to-end systems.

In this work, we propose an approach to learn task graphs from demonstrations in the form of sequences of key-steps performed by real users in a video while executing a procedure. Given a directed graph represented as an adjacency matrix and a set of key-step sequences, we provide an estimate of the likelihood of observing the set of sequences given the constraints encoded in the graph. We hence formulate task graph learning under the well-understood framework of Maximum Likelihood (ML) estimation, and propose a novel differentiable Task Graph Maximum Likelihood (TGML) loss function which can be naturally plugged into any neural-based architecture for direct optimization of task graph from data. Intuitively, our TGML loss generates positive gradients to strengthen the weights of directed edges $B \to A$ when observing the $< \dots, A, \dots, B, \dots >$ structure, while pushing down the weights of all other edges in a contrastive manner (see Figure 1(b). To evaluate the effectiveness of the proposed framework, we propose two approaches to task graph learning. The first approach, "Direct Optimization (DO)" uses the proposed TGML loss to directly optimize the weights of the adjacency matrix, which constitute the only parameters of the model. The output of the optimization procedure is the learned graph. The second approach, termed Task Graph Transformer (TGT) is a feature-based model which uses a transformer encoder and a relation head to predict the adjacency matrix from either text or video key-step embeddings.

We validate the ability of our framework to learn meaningful task graphs on the CaptainCook4D dataset [26]. Comparisons with state-of-the-art approaches show superior performance of both proposed approaches on task graph generation, with boosts of up to +16.7% over prior methods. On the same dataset, we show that our feature-based approach implicitly gains video understanding abilities on two fundamental tasks [42]: pairwise ordering and future prediction. We finally assess the usefulness of the learned graph-based representation on the downstream task of online mistake detection in procedural egocentric videos. To tackle this task, we observe that procedural errors mainly arise from the execution of a given key-step without the correct execution of its pre-conditions. We hence design an approach which uses the learned graph to check whether pre-conditions for the current action are satisfied, signaling a mistake when they are not, obtaining significant gains of +19.8% and +7.5% in the online mistake detection benchmark recently introduced in [12] on Assembly101 [33] and EPIC-Tent [17], showcasing the relevance and quality of the learned graph-based representations.

The contributions of this work are: 1) We introduce a novel framework for learning *task graphs* from action sequences, which relies on maximum likelihood estimation to provide a differentiable loss function which can be included in end-to-end models and optimized with gradient descent; 2)

We propose two approaches to task graph learning based on direct optimization of the adjacency matrix and processing key-step text or video embeddings, which offer significant improvements over previous methods in task graph generation and shows emerging video understanding abilities; 3) We showcase the usefulness of task graphs in general, and the learned graph-based representations in particular, on the downstream task of online mistake detection from video, where we improve over competitors. The code to replicate the experiments is available at https://github.com/fpv-iplab/Differentiable-Task-Graph-Learning.

2 Related Work

Procedure Understanding Previous investigations considered different tasks related to procedure understanding, such as inferring key-steps from video in an unsupervised way [41, 43, 11, 4, 5, 10], grounding key-steps in procedural video [22, 8, 9, 24], recognizing the performed procedure [21], inferring key-step orderings [4, 5, 22, 9, 39], and procedure structure verification [25]. Recently, task graphs, mined from video or external knowledge such as WikiHow articles, have been investigated as a powerful representation of procedures and proved advantageous for learning representations useful for downstream tasks such as key-step recognition and forecasting [40, 3].

Differently from previous works [25, 39], we aim to develop an explicit and human readable representation of the procedure which can be directly plugged in to enable downstream tasks [3], rather than an implicit representation obtained with pre-training objective [40, 25]. As a departure from previous paradigms which carefully designed task graph construction procedures [3, 40, 35, 18], we frame task prediction in a general learning framework, enabling models to learn task graphs directly from input sequences, and propose a differentiable loss function based on maximum likelihood.

Task Graph Construction A line of works investigated the construction of task graphs from natural language descriptions of procedures (e.g., recipes) using rule-based graph parsing [32, 9], defining probabilistic models [20], fine-tuning language models [31], or proposing learning-based approaches [9] involving parsers and taggers trained on text corpora of recipes [7, 38]. While these approaches do not require any action sequence as input, they depend on the availability of text corpora including procedural knowledge, such as recipes, which often fail to encapsulate the variety of ways in which the procedure may be executed [3]. Other works proposed hand-crafted approaches to infer task graphs observing sequences of actions depicting task executions [18, 35]. Recent work designed procedures to mine task graphs from videos and textual descriptions of key-steps [3] or cross-referencing visual and textual representations from corpora of procedural text and videos [40].

Differently from previous efforts, we rely on action sequences, grounded in video, rather than natural language descriptions of procedures or recipes [31, 9] and frame task graph generation as a learning problem, providing a differentiable objective rather than resorting to hand-designed algorithms and task extraction procedures [18, 35, 3, 40].

Online Mistake Detection in Procedural Videos Despite the interest in procedural learning, mistake detection has been systematically investigated only recently. Some methods considered fully supervised scenarios in which mistakes are explicitly labeled in video and mistake detection is performed offline [33, 37, 26]. Other approaches considered weak supervision, with mistakes being labeled only at the video level [14]. Finer-grade spatial and temporal annotations are exploited in [6] to build knowledge graphs, which are then leveraged to perform mistake detection. Recently, the authors of [12] proposed an online mistake detection benchmark incorporating videos from the Assembly101 [33] and EPIC-Tent [17] datasets, as well as PREGO, an approach to online mistake detection in procedural egocentric videos.

Rather than addressing online mistake detection with implicit representations [12] or carefully designed knowledge bases [33], we design a simple approach which relies on learned explicit task graph representations. As we show in the experiments, this leads to obtain significant performance gains over previous methods, even when the predicted graphs are suboptimal, while best results are obtained with task graphs learned within the proposed framework.

3 Technical Approach

3.1 Task Graph Maximum Likelihood Learning Framework

Preliminaries Let $\mathcal{K} = \{K_0 = S, K_1, \dots, K_n, K_{n+1} = E\}$ be the set of key-steps involved in the procedure, where S and E are placeholder "start" and "end" key-steps denoting the start and end of the procedure. We define the task graph as a directed acyclic graph, i.e., a tuple $G = (\mathcal{K}, \mathcal{A}, \omega)$, where \mathcal{K} is the set of nodes (the key-steps), $\mathcal{A} = \mathcal{K} \times \mathcal{K}$ is the set of possible directed edges indicating ordering constraints between pairs of key-steps, and $\omega: \mathcal{A} \to [0,1]$ is a function assigning a score to each of the edges in \mathcal{A} . An edge $(K_i, K_j) \in \mathcal{A}$ (also denoted as $K_i \to K_j$) indicates that K_j is a pre-condition of K_i (for instance mix \to crack egg) with score $\omega(K_i, K_j)$. We assume normalized weights for outgoing edges, i.e., $\sum_j w(K_i, K_j) = 1 \forall i$. We also represent the graph G as the adjacency matrix $Z \in [0,1]^{n \times n}$, where $Z_{ij} = \omega(K_i, K_j)$. For ease of notation, we will denote the graph $G = (\mathcal{K}, \mathcal{A}, \omega)$ simply with its adjacency matrix Z in the rest of the paper. We assume that a set of N sequences $\mathcal{Y} = \{y^{(k)}\}_{k=1}^N$ showing possible orderings of the key-steps \mathcal{K} is available, where the generic sequence $y \in \mathcal{Y}$ is defined as a set of indexes to key-steps \mathcal{K} , i.e., $y = \langle y_0, \dots, y_t, \dots, y_{m+1} \rangle$, with $y_t \in \{0, \dots, n+1\}$. We further assume that each sequence starts with key-step S and ends with key-step E, i.e., $y_0 = 0$ and $y_{m+1} = n+1^1$ and note that different sequences $y^{(i)}$ and $y^{(j)}$ have in general different lengths. Since we are interested in modeling key-step orderings, we assume that sequences do not contain repetitions. We frame task graph learning as determining an adjacency matrix \hat{Z} such that sequences in \mathcal{Y} can be seen as topological sorts of \hat{Z} . A principled way to approach this problem is to provide an estimate of the likelihood $P(\mathcal{Y}|Z)$ and choose the maximum likelihood estimate $\hat{Z} = \arg\max_i P(\mathcal{Y}|Z)$.

Modeling Sequence Likelihood for an Unweighted Graph Let us consider the special case of an unweighted graph, i.e., $\bar{Z} \in \{0,1\}^{n \times n}$. We wish to estimate P(y|Z), the likelihood of the generic sequence $y \in \mathcal{Y}$ given graph Z. Formally, let Y_t be the random variable related to the event "key-step K_{y_t} appears at position t in sequence y". We can factorize the conditional probability P(y|Z) as:

$$P(y|Z) = P(Y_0, \dots, Y_{|y|}|Z) = P(Y_0|Z) \cdot P(Y_1|Y_0, Z) \cdot \dots \cdot P(Y_{|y|}|Y_0, \dots, Y_{|y|-1}, Z).$$
(1)

We assume that the probability of observing a given key-step K_{y_t} at position t in y depends on the previously observed key-steps $(K_{y_{t-1}},\ldots,K_{y_0})$, but not on their ordering, i.e., the probability of observing a given key-step depends on whether its pre-conditions are satisfied, regardless of the order in which they have been satisfied. Under this assumption, we write $P(Y_t|Y_{t-1},\ldots,Y_0,Z)$ simply as $P(K_{y_t}|K_{y_{t-1}},\ldots,K_{y_0},Z)$. Without loss of generality, in the following, we denote the current key-step as $K_i = K_{y_t}$, the indexes of key-steps observed at time t as $\mathcal{J} = \mathcal{O}(y,t) = \{y_{t-1},\ldots,y_0\}$, and the corresponding set of observed key-steps as $K_{\mathcal{J}} = \{K_i|i\in\mathcal{J}\}$. Similarly, we define $\bar{\mathcal{J}} = \overline{\mathcal{O}(y,t)} = \{0,\ldots,n+1\} \setminus \mathcal{O}(y,t)$ and $K_{\bar{\mathcal{J}}}$ as the sets of indexes and corresponding key-steps unobserved at position t, i.e., those which do not appear before y_t in the sequence. Given the factorization above, we are hence interested in estimating the general term $P(K_{y_t}|K_{y_{t-1}},\ldots,K_{y_0}) = P(K_i|K_{\mathcal{J}})$. We can estimate the probability of observing key-step K_i given the set of observed key-steps $K_{\mathcal{J}}$ and the constraints imposed by \bar{Z} , following Laplace's classic definition of probability [23] as "the ratio of the number of favorable cases to the number of possible cases". Specifically, if we were to randomly sample a key-step from K following the constraints of \bar{Z} , and having observed key-steps $K_{\mathcal{J}}$, sampling K_i would be a favorable case if all pre-conditions of K_i were satisfied, i.e., if $\sum_{j\in\bar{\mathcal{J}}} Z_{ij} = 0$ (there are no pre-conditions in unobserved key-steps $K_{\bar{\mathcal{J}}}$). Similarly, sampling a key-steps K_i is a "possible case" if $\sum_{j\in\bar{\mathcal{J}}} Z_{hj} = 0$. We can hence define the probability of observing key-steps K_i after observing all key-steps $K_{\mathcal{J}}$ in a sequence as follows:

$$P(K_i|K_{\mathcal{J}}, \bar{Z}) = \frac{\text{number of favorable cases}}{\text{number of possible cases}} = \frac{\mathbb{1}(\sum_{j \in \bar{\mathcal{J}}} \bar{Z}_{ij} = 0)}{\sum_{h \in \bar{\mathcal{J}}} \mathbb{1}(\sum_{j \in \bar{\mathcal{J}}} \bar{Z}_{hj} = 0)}$$
(2)

where $\mathbb{1}(\cdot)$ denotes the indicator function, and in the denominator, we are counting the number of key-steps that have not appeared yet are "possible cases" under the given graph Z. Likelihood P(y|Z) can be obtained by plugging Eq. (2) into Eq. (1).

 $^{^{1}}$ In practice, we prepend/append S and E to each sequence.

²Since sequences may in practice contain repetitions, we map each sequence containing repetitions to multiple sequences with no repetitions (e.g., $ABCAD \rightarrow (ABCD, BCAD)$).

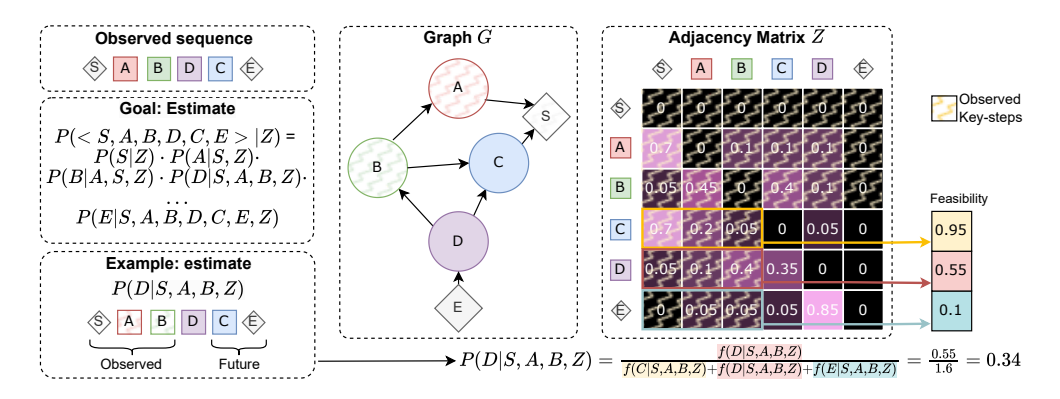


Figure 2: Given a sequence < S, A, B, D, C, E>, and a graph G with adjacency matrix Z, our goal is to estimate the likelihood P(< S, A, B, C, D, E>|Z|), which can be done by factorizing the expression into simpler terms. The figure shows an example of computation of probability P(D|S,A,B,Z) as the ratio of the "feasibility of sampling key-step D, having observed key-steps S, A, and B" to the sum of all feasibility scores for unobserved symbols. Feasibility values are computed by summing weights of edges $D \to X$ for all observed key-steps X.

Modeling Sequence Likelihood for a Weighted Graph In practice, to enable gradient-based learning, we consider the general case of a continuous adjacency matrix $Z \in [0,1]^{n \times n}$. We generalize the concept of "possible cases" discussed in the previous section with the concept of "feasibility of sampling a given key-step K_i , having observed a set of key-steps $K_{\mathcal{J}}$, given graph Z", which we define as the sum of all weights of edges between observed key-steps $K_{\mathcal{J}}$ and K_i : $f(K_i|K_{\mathcal{J}},Z) = \sum_{j \in \mathcal{J}} Z_{ij}$. Intuitively, if key-step k_i has many satisfied pre-conditions, we are more likely to sample it as the next key-step. We hence define $P(K_i|K_{\mathcal{J}},Z)$ as "the ratio of the feasibility of sampling K_i to the sum of the feasibilities of sampling any unobserved key-step":

$$P(K_i|K_{\mathcal{J}},Z) = \frac{f(K_i|K_{\mathcal{J}},Z)}{\sum_{h\in\bar{\mathcal{J}}} f(K_h|K_{\mathcal{J}},Z)} = \frac{\sum_{j\in\mathcal{J}} Z_{ij}}{\sum_{h\in\bar{\mathcal{J}}} \sum_{j\in\mathcal{J}} Z_{hj}}$$
(3)

Figure 2 illustrates the computation of the likelihood in Eq. 3. Plugging Eq. (3) into Eq. (1), we can estimate the likelihood of a sequence y given graph Z as:

$$P(y|Z) = P(S|Z) \prod_{t=1}^{|y|} P(K_{y_t}|K_{\mathcal{O}(y,t)}, Z) = \prod_{t=1}^{|y|} \frac{\sum_{j \in \mathcal{O}(y,t)} Z_{y_t j}}{\sum_{h \in \overline{\mathcal{O}(y,t)}} \sum_{j \in \mathcal{O}(y,t)} Z_{hj}}.$$
 (4)

Where we set $P(K_{y_0}|Z) = P(S|Z) = 1$ as sequences always start with the start node S

Task Graph Maximum Likelihood Loss Function Assuming that sequences $y^{(i)} \in \mathcal{Y}$ are independent and identically distributed, we define the likelihood of \mathcal{Y} given graph Z as follows:

$$P(\mathcal{Y}|Z) = \prod_{k=1}^{|\mathcal{Y}|} P(y^{(k)}|Z) = \prod_{k=1}^{|\mathcal{Y}|} \prod_{t=1}^{|\mathcal{Y}|} \frac{\sum_{j \in \mathcal{O}(y^{(k)}, t)} Z_{y_t j}}{\sum_{h \in \overline{\mathcal{O}(y^{(k)}, t)}} \sum_{j \in \mathcal{O}(y^{(k)}, t)} Z_{h j}}.$$
 (5)

We can find the optimal graph Z by maximizing the likelihood in Eq. (5), which is equivalent to minimizing the negative log-likelihood $-\log P(\mathcal{Y}, Z)$, leading to formulating the following loss:

where β is a hyper-parameter. We refer to Eq. (6) as the *Task Graph Maximum Likelihood (TGML)* loss function. Since Eq. (6) is differentiable with respect to all Z_{ij} values, we can learn the adjacency matrix Z by minimizing the loss with gradient descent to find the estimated graph $\hat{Z} = \arg_Z \max \mathcal{L}(\mathcal{Y}, Z)$. Eq. (6) works as a contrastive loss in which the first logarithmic term aims

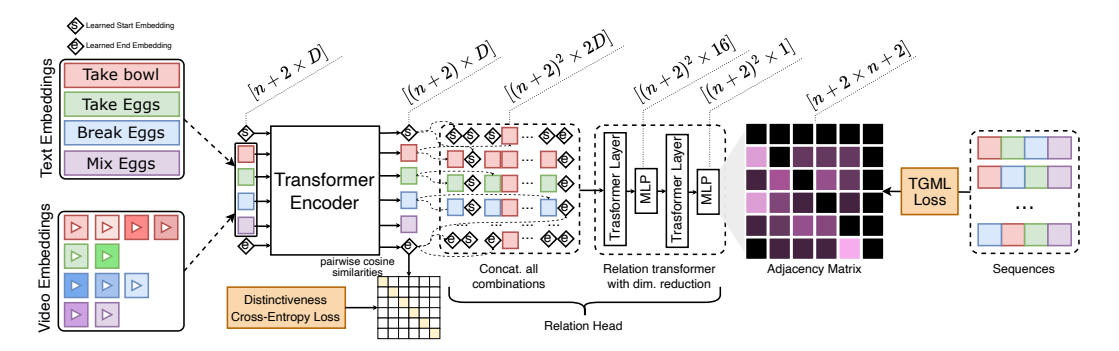


Figure 3: Our Task Graph Transformer (TGT) takes as input either D-dimensional text embeddings or video embeddings extracted from key-step segments. Learnable S and E embeddings are also included. Key-step embeddings are processed with a transformer encoder and regularized with a distinctiveness cross-entropy to prevent representation collapse. Output embeddings are processed with our relation head which concatenates vectors across all $(n+2)^2$ possible node pairs, thus obtaining $(n+2)\times(n+2)\times 2D$ relation vectors. These are processed by a relation transformer which progressively maps relation vectors to an $(n+2)\times(n+2)$ adjacency matrix. The model is supervised with input sequences using our proposed Task Graph Maximum Likelihood (TGML) loss.

to maximize, at every step t of each input sequence, the weights Z_{y_tj} of edges $K_{y_t} \to K_j$ going from the current key-step K_{y_t} to all previously observed key-steps K_j , while the second logarithmic term (contrastive term) aims to minimize the weights of edges $K_h \to K_j$ between key-steps yet to appear K_h and already observed key-steps K_j . The hyper-parameter β regulates the influence of the summation in the contrastive term which, including many more addends, can dominate gradient updates.

3.2 Models

Direct Optimization (DO) The first model aims to directly optimize the parameters of the adjacency matrix by performing gradient descent on the TGML loss (Eq. (6)). We define the parameters of this model as an edge scoring matrix $A \in \mathbb{R}^{(n+2)\times (n+2)}$, where n is the number of key-steps, plus the placeholder start (S) and end (E) nodes, and A_{ij} is a score assigned to edge $K_i \to K_j$. To prevent the model from learning edge weights eluding the assumptions of directed acyclic graphs, we mask black cells in Figure 2 with $-\infty$. To constrain the elements of Z in the [0,1] range and obtain normalized weights, we softmax-normalize the rows of the scoring matrix to obtain the adjacency matrix Z = softmax(A). Note that elements masked with $-\infty$ will be automatically mapped to 0 by the softmax function similarly to [36]. We train this model by performing batch gradient descent directly on the score matrix A with the proposed TGML loss. We train a separate model per procedure, as each procedure is associated to a different task graph. As many applications require an unweighted graph, we binarize the adjacency matrix with the threshold $\frac{1}{n}$, where n is the number of nodes. We also employ a post-processing stage in which we remove redundant edges, loops, and add obvious missing connections to S and E nodes.

Task Graph Transformer (TGT) Figure 3 illustrates the proposed model, which is termed Task Graph Transformer (TGT). The proposed model can take as input either D-dimensional embeddings of textual descriptions of key-steps or D-dimensional video embeddings of key-step segments extracted from video. In the first case, the model takes as input the same set of embeddings at each forward pass, while in the second case, at each forward pass, we randomly sample a video embedding per key-step from the training videos (hence each key-step embedding can be sampled from a different video). We also include two D-dimensional learnable embeddings for the S and E nodes. All key-step embeddings are processed by a transformer encoder, which outputs D-dimensional vectors enriched with information from other embeddings. To prevent representation collapse, we apply a regularization loss encouraging distinctiveness between pairs of different nodes. Let X be the matrix of embeddings produced by the transformer model. We L2-normalize features, then compute

³See the supplementary material for more details.

Table 1: Task graph generation results on CaptainCook4D. Table 2: We compare the abilities of our Best results are in **bold**, second best results are <u>underlined</u>, TGT model trained on visual features best results among competitors are <u>highlighted</u>. Confitogeneralize to two fundamental video dence interval bounds computed at 95% conf. for 5 runs. understanding tasks, i.e., pairwise order-

Method	Precision	Recall	F_1
MSGI [35] LLM	11.9 52.9	14.0 57.4	12.8 55.0
Count-Based [3]	66.9	56.1	61.0
MSG ² [18]	70.9	71.6	71.1
TGT-text (Ours) DO (Ours)	$\frac{71.7}{86.4} \pm 3.6$	$\frac{72.9}{89.7}$ ±2.8	$\frac{72.1}{87.8} \pm 3.2$
Improvement	+15.5	+18.1	+16.7

Table 2: We compare the abilities of our TGT model trained on visual features to generalize to two fundamental video understanding tasks, i.e., pairwise ordering and future prediction. Despite not being explicitly trained for these tasks, our model exhibits video understanding abilities, surpassing the baseline.

Method	Ordering	Fut. Pred.
Random	50.00	50.00
TGT-video	63.11	62.19
Improvement	+13.11	+12.19

pairwise cosine similarities $Y=X\cdot X^T\cdot \exp(T)$ as in [29]. To prevent the transformer encoder from mapping distinct key-step embeddings to similar representations, we enforce the values outside the diagonal of Y to be smaller than the values in the diagonal. This is done by encouraging each row of the matrix Y to be close to a one-hot vector with a cross-entropy loss. Regularized embeddings are finally passed through a relation transformer head which considers all possible pairs of embeddings and concatenates them in a $(n+2)\times (n+2)\times 2D$ matrix R of relation vectors. For instance, R[i,j] is the concatenation of vectors X[i] and X[j]. Relation vectors are passed to a transformer layer which aims to mine relationships among relation vectors, followed by a multilayer perceptron to reduce dimensionality to 16 units and another pair of transformer layer and multilayer perceptron to map relation vectors to scalar values, which are reshaped to size $(n+2)\times (n+2)$ to form the score matrix A. We hence apply the same optimization procedure as in the DO method to supervise the whole architecture.

4 Experiments and Results

4.1 Graph Generation

Problem Setup We evaluate the ability of our approach to learn task graph representations on CaptainCook4D [26], a dataset of egocentric videos of 24 cooking procedures performed by 8 volunteers. Each procedure is accompanied by a task graph describing key-steps constraints. We tackle task graph generation as a weakly supervised learning problem in which models have to generate valid graphs by only observing labeled action sequences (weak supervision) rather than relying on task graph annotations (strong supervision), which are not available at training time. All models are trained on videos that are free from ordering errors or missing steps to provide a likely representation of procedures. We use the two proposed methods in the previous section to learn 24 task graph models, one per procedure, and report average performance across procedures.

Compared Approaches We compare our methods with previous approaches to task graph generation, and in particular with MSGI [35] and MSG² [18], which are approaches for task graph generation based on Inductive Logic Programming (ILP). We also consider the recent approach proposed in [3] which generates a graph by counting co-occurrences of matched video segments. Since we assume labeled actions to be available at training time, we do not perform video matching and use ground truth segment matching provided by the annotations. This approach is referred to as "Count-Based". Given the popularity of large language models as reasoning modules, we also consider a baseline which uses a large language model⁴ to generate a task graph from key-step descriptions, without any access to key-step sequences.⁵ We refer to this model as "LLM".

Graph Generation Results Results in Table 1 highlight the complexity of the task, with classic approaches based on inductive logic, such as MSGI, achieving poor performance (12.8 F_1), language models and count-based statistics reconstructing only basic elements of the graph (55.0 and 61.0 F_1 for LLM and Count-Based respectively), and even more recent methods based on inductive logic and heuristics only partially predicting the graph (71.1 F_1 of MSG^2). The proposed Direct Optimization

⁴We base our experiments on ChatGPT [1].

(DO) approach outperforms all other methods, achieving the highest scores across all measures, with improvements in the [+15.5, +18.1] range with respect to the best competitor MSG^2 . This result highlights the effectiveness of the proposed framework to learn task graph representations from key-step sequences, especially considering the simplicity of the DO method, which performs gradient descent directly on the adjacency matrix. We obtain a slightly higher recall as compared to the precision (89.7 vs 86.4), showing that our approach tends to retrieve most ground truth edges, while hallucinating some pre-conditions, probably due to the dataset being unbalanced towards the most common ways of completing a procedure. Second best results are consistently obtained by our feature-based TGT approach, showing the generality of our learning framework and the potential of integrating it into complex neural architectures. Tight confidence intervals for DO highlight the stability of the proposed loss. The lower performance of TGT, as compared to DO, may be due to the relatively small size of the dataset, which makes it hard for complex architecture to generalize.

Video Understanding Results Table 2 reports the performance of TGT trained on videos on two fundamental video understanding tasks [42] of pairwise clip ordering and future prediction. For pairwise ordering, we feed our TGT model with video embeddings of two clips and sort them according to the predicted adjacency matrix, placing first the clip identified as a pre-condition. For future predictions, given an anchor clip, we have to choose which among two other clips is the correct future. In this case, we feed the model with the three clips and select as future the clip with the smallest $anchor \rightarrow clip$ edge weight (future clips are not likely pre-conditions). Despite TGT not being explicitly trained for pairwise ordering and future predictions, it exhibits promising emerging video understanding abilities, surpassing the random baseline.

4.2 Online Mistake Detection

Problem Setup We follow the PREGO benchmark recently proposed in [12], in which models are tasked to perform online action detection from procedural egocentric videos. To evaluate the usefulness of task graphs on this downstream task, we design a system which flags the current action as a mistake if its pre-conditions in the predicted graph do not appear in previously observed actions.⁵

Competitors We compare our approach with respect to the PREGO model proposed in [12], which detects mistakes based on the comparison between the currently observed action and an action predicted by a forecasting module. We note that PREGO is based on an implicit representation of the procedure (the forecasting module), while our approach is based on the explicit task graph representation, learned with the proposed framework. We also compare our approach with respect to baselines based on all graph prediction approaches compared in Table 1 to assess how the ability to predict accurate graphs affects downstream performance. For all methods, we report results based on ground truth action segments and on action sequences predicted by a MiniRoad [2] instance, a state-of-the-art online action detection module trained on each target dataset.

Results Results in Table 3 highlight the usefulness of the learned task graphs for downstream applications. The proposed DO method achieves significant gains over prior art with improvements of +19.8 and +7.5 in average F_1 score on Assembly 101 and EPIC-Tent respectively when ground truth action sequences are considered to make predictions. While TGT is the second-best performer on Assembly 101, it obtains best results on EPIC-Tent (64.1 vs 58.3 in average F_1 score). This is due to the nature of action annotations in the two datasets. Indeed, while key-step names are informative in EPIC-Tent (e.g., "Place Vent Cover", "Open Stake Bag", or "Spread Tent"), they are less distinctive in Assembly101 (e.g., "attach cabin", "attach interior", or "screw chassis"). This highlights the flexibility of the proposed learning framework which can work in purely abstract, symbolic settings, with the DO approach, but can also leverage semantics with TGT when beneficial. Interestingly, the second best performers are graph-based approaches, with MSG^2 achieving an average F_1 of 56.1 on Assembly 101 and the simple Count-Based approach obtaining an average F_1 score of 56.6on EPIC-Tent. In contrast, PREGO obtains average F_1 scores of 39.4 and 32.1 on Assembly 101 and EPIC-Tent respectively, suggesting the potential of explicit graph-based representations for mistake detection, versus the implicit one of PREGO. Breaking down performance into correct and mistake F_1 scores reveal some degree of unbalance of our approaches and the main competitor MSG^2 towards identifying correct actions rather than mistakes. This suggests that the related graph-based representations tend to detect some spurious pre-conditions, probably due to the limited demonstrations included in the videos, while the implicit PREGO model exhibits a skew with respect

⁵See the supplementary material for more details.

Table 3: Online mistake detection results. Results obtained with ground truth action sequences are denoted with *, while results obtained on predicted action sequences are denoted with +.

	Assembly101			EPIC-Tent										
	Avg	Co	orrect		Mi	istake	;	Avg	C	orrec	t	Mi	stake	;
Method	$\overline{F_1}$	$\overline{F_1}$	Prec	Rec	$\overline{F_1}$	Prec	Rec	$\overline{F_1}$	$\overline{F_1}$	Prec	Rec	$\overline{F_1}$	Prec	Rec
Count-Based* [3]	26.2	9.5	5.1	86.2	42.9	97.8	27.5	56.6	92.5	92.8	92.2	20.7	20.0	21.4
LLM^*	29.3	15.1	8.3	87.2	43.4	96.7	27.9	47.7	86.3	82.4	90.6	9.1	13.3	6.9
MSGI* [35]	33.1	22.7	13.1	84.4	43.5	93.4	28.3	44.5	66.9	51.6	95.2	22.0	73.3	12.9
PREGO* [12]	39.4	32.6	89.7	19.9	46.3	30.7	94.0	32.1	45.0	95.7	29.4	19.1	10.7	86.7
MSG^{2*} [18]	56.1	63.9	51.5	84.2	48.2	73.6	35.8	54.1	92.9	94.1	91.7	15.4	13.3	18.2
TGT-text (Ours)*	62.8	69.8	56.8	90.6	<u>55.7</u>	84.1	41.7	64.1	93.8	94.1	93.5	34.5	33.3	35.7
DO (Ours)*	75.9	90.2	98.2	83.4	61.6	46.7	90.4	<u>58.3</u>	<u>93.5</u>	94.8	92.4	<u>23.1</u>	20.0	27.3
Improvement*	+19.8	+26.3			+13.4			+7.5	+0.9			+12.5		
Count-Based ⁺ [3]	23.1	2.5	1.3	60.0	43.7	97.8	28.1	38.1	68.3	54.9	90.1	7.9	26.7	4.7
LLM^+	28.1	15.1	7.8	65.5	42.3	89.5	27.7	35.9	61.6	46.7	90.4	10.2	40.0	5.8
MSGI ⁺ [35]	28.4	14.0	7.8	67.9	<u>42.7</u>	90.7	28.0	40.4	59.2	42.9	95.5	21.6	80.0	12.5
PREGO ⁺ [12]	32.5	23.1	68.8	13.9	41.8	27.8	84.1	29.4	41.6	97.9	26.4	17.2	9.5	93.3
MSG^{2+} [18]	46.2	59.1	51.2	70.0	33.2	44.5	26.5	45.2	67.5	52.4	95.1	22.9	73.3	13.6
TGT-text (Ours) ⁺	53.0	<u>67.8</u>	62.3	74.5	38.2	46.2	32.6	43.8	69.5	55.8	92.1	18.2	53.3	11.0
DO (Ours) ⁺	53.5	78.9	85.0	73.5	28.1	22.5	37.3	46.5	<u>69.3</u>	54.4	95.2	23.7	73.3	14.1
Improvement ⁺	+7.3	+19.8			-5.5			+1.3	+1.2			+1.2		

to mistakes. Further breaking down F_1 scores into related precision and recall values highlights that the main failure modes are due to large imbalances between precision and recall. For instance, the Count-Based method achieves a precision of only 5.1 with a recall of 86.2 in predicting correct segments on Assembly 101. In contrast, the proposed approach obtains balanced precision and recall values in detecting correct segments in Assembly 101 (98.2/83.4) and EPIC-Tent (94.8/92.4), and detecting mistakes in EPIC-Tent (33.2/35.7), while the prediction of mistakes on Assembly101 is more skewed (46.7/90.4). Results based on action sequences predicted from video (bottom part of Table 3) highlight the challenging nature of the task, when considering noisy action sequences. While the explicit task graph representation may not accurately reflect the predicted noisy action sequences, we still observe improvements over previous approaches of +7.3 and +1.3 in average F_1 score in Assembly101 and EPIC-Tent. Remarkably, best competitors are still graph-based methods, such as MSG^2 and the Count-Based approach, with significant improvements over the implicit representation of the PREGO model (32.5 average F_1 versus 53.5 of the proposed DO model). Also in this case, we observe that graph-based methods tend to be skewed towards detecting correct action sequences. In this regard, our TGT model only achieves 38.2 mistake F_1 score, a drop in 5.5 points over the best performer, the Count-Based method, which, on the other hand, only achieves an F_1 score of 2.5 when predicting correct segments.

5 Limitations

The proposed approach requires the availability of key-step sequences, a common assumption of works addressing other video understanding tasks such as action recognition. While our method is applicable to any fully supervised video understanding dataset, future works should focus on overcoming such limitation and taking advantage of the vast amount of unlabeled video and textual data sets. While the proposed TGT method has shown promising results when trained directly on video features, the investigation of task graph learning in the absence of labeled key-step sequences is beyond the scope of this paper. We noted a reduced ability of our approach to work with noisy action sequences and a tendency to hallucinate pre-conditions, likely due to the limited expressivity of key-steps sequences arising from videos showing the most common ways to perform a procedure.

6 Conclusion

We considered the problem of learning task graph representations of procedures from video demonstrations. Framing task graph learning as a maximum likelihood estimation problem, we proposed a differentiable loss which allows direct optimization of the adjacency matrix through gradient descent and can be plugged into more complex neural network architectures. Experiments on three datasets show that the proposed approach can learn accurate task graphs, develop video understanding abilities, and improve the downstream task of online mistake detection surpassing state of the art methods. We release our code at the following URL: https://github.com/fpv-iplab/Differentiable-Task-Graph-Learning.

7 Acknowledgments

This research is supported in part by the PNRR PhD scholarship "Digital Innovation: Models, Systems and Applications" DM 118/2023, by the project Future Artificial Intelligence Research (FAIR) – PNRR MUR Cod. PE0000013 - CUP: E63C22001940006, and by the Research Program PIAno di inCEntivi per la Ricerca di Ateneo 2020/2022 — Linea di Intervento 3 "Starting Grant" EVIPORES Project - University of Catania.

We thank the authors of [12] and in particular Alessandro Flaborea and Guido D'Amely for sharing the code to replicate experiments in the PREGO benchmark.

References

- [1] Josh Achiam, Steven Adler, Sandhini Agarwal, Lama Ahmad, Ilge Akkaya, Florencia Leoni Aleman, Diogo Almeida, Janko Altenschmidt, Sam Altman, Shyamal Anadkat, et al. Gpt-4 technical report. *arXiv* preprint arXiv:2303.08774, 2023.
- [2] Joungbin An, Hyolim Kang, Su Ho Han, Ming-Hsuan Yang, and Seon Joo Kim. Miniroad: Minimal rnn framework for online action detection. In *Proceedings of the IEEE/CVF International Conference on Computer Vision*, pages 10341–10350, 2023.
- [3] Kumar Ashutosh, Santhosh Kumar Ramakrishnan, Triantafyllos Afouras, and Kristen Grauman. Videomined task graphs for keystep recognition in instructional videos. Advances in Neural Information Processing Systems, 36, 2024.
- [4] Siddhant Bansal, Chetan Arora, and CV Jawahar. My view is the best view: Procedure learning from egocentric videos. In *European Conference on Computer Vision*, pages 657–675. Springer, 2022.
- [5] Siddhant Bansal, Chetan Arora, and CV Jawahar. United we stand, divided we fall: Unitygraph for unsupervised procedure learning from videos. In *Proceedings of the IEEE/CVF Winter Conference on Applications of Computer Vision*, pages 6509–6519, 2024.
- [6] Guodong Ding, Fadime Sener, Shugao Ma, and Angela Yao. Every mistake counts in assembly. *arXiv* preprint arXiv:2307.16453, 2023.
- [7] Lucia Donatelli, Theresa Schmidt, Debanjali Biswas, Arne Köhn, Fangzhou Zhai, and Alexander Koller. Aligning actions across recipe graphs. In *Proceedings of the 2021 conference on empirical methods in natural language processing*, pages 6930–6942, 2021.
- [8] Mikita Dvornik, Isma Hadji, Konstantinos G Derpanis, Animesh Garg, and Allan Jepson. Drop-dtw: Aligning common signal between sequences while dropping outliers. *Advances in Neural Information Processing Systems*, 34:13782–13793, 2021.
- [9] Nikita Dvornik, Isma Hadji, Hai Pham, Dhaivat Bhatt, Brais Martinez, Afsaneh Fazly, and Allan D Jepson. Graph2vid: Flow graph to video grounding for weakly-supervised multi-step localization. In *Proceedings* of the European Conference on Computer Vision (ECCV), 2022.
- [10] Nikita Dvornik, Isma Hadji, Ran Zhang, Konstantinos G Derpanis, Richard P Wildes, and Allan D Jepson. Stepformer: Self-supervised step discovery and localization in instructional videos. In *Proceedings of the IEEE/CVF Conference on Computer Vision and Pattern Recognition*, pages 18952–18961, 2023.
- [11] Ehsan Elhamifar and Dat Huynh. Self-supervised multi-task procedure learning from instructional videos. In *Computer Vision–ECCV 2020: 16th European Conference, Glasgow, UK, August 23–28, 2020, Proceedings, Part XVII 16*, pages 557–573. Springer, 2020.

- [12] Alessandro Flaborea, Guido Maria D'Amely di Melendugno, Leonardo Plini, Luca Scofano, Edoardo De Matteis, Antonino Furnari, Giovanni Maria Farinella, and Fabio Galasso. Prego: online mistake detection in procedural egocentric videos. In *International Conference on Computer Vision and Patter Recognition (CVPR)*, 2024.
- [13] Antonino Furnari and Giovanni Maria Farinella. Rolling-unrolling lstms for action anticipation from first-person video. *IEEE transactions on pattern analysis and machine intelligence*, 43(11):4021–4036, 2020.
- [14] Reza Ghoddoosian, Isht Dwivedi, Nakul Agarwal, and Behzad Dariush. Weakly-supervised action segmentation and unseen error detection in anomalous instructional videos. In *Proceedings of the IEEE/CVF International Conference on Computer Vision*, pages 10128–10138, 2023.
- [15] Rohit Girdhar and Kristen Grauman. Anticipative video transformer. In Proceedings of the IEEE/CVF international conference on computer vision, pages 13505–13515, 2021.
- [16] Kristen Grauman, Andrew Westbury, Lorenzo Torresani, Kris Kitani, Jitendra Malik, Triantafyllos Afouras, Kumar Ashutosh, Vijay Baiyya, Siddhant Bansal, Bikram Boote, et al. Ego-exo4d: Understanding skilled human activity from first-and third-person perspectives. *arXiv preprint arXiv:2311.18259*, 2023.
- [17] Youngkyoon Jang, Brian Sullivan, Casimir Ludwig, Iain Gilchrist, Dima Damen, and Walterio Mayol-Cuevas. Epic-tent: An egocentric video dataset for camping tent assembly. In *Proceedings of the IEEE/CVF International Conference on Computer Vision Workshops*, pages 0–0, 2019.
- [18] Yunseok Jang, Sungryull Sohn, Lajanugen Logeswaran, Tiange Luo, Moontae Lee, and Honglak Lee. Multimodal subtask graph generation from instructional videos. arXiv preprint arXiv:2302.08672, 2023.
- [19] Takeo Kanade and Martial Hebert. First-person vision. *Proceedings of the IEEE*, 100(8):2442–2453, 2012.
- [20] Chloé Kiddon, Ganesa Thandavam Ponnuraj, Luke Zettlemoyer, and Yejin Choi. Mise en place: Unsupervised interpretation of instructional recipes. In *Proceedings of the 2015 Conference on Empirical Methods in Natural Language Processing*, pages 982–992, 2015.
- [21] Xudong Lin, Fabio Petroni, Gedas Bertasius, Marcus Rohrbach, Shih-Fu Chang, and Lorenzo Torresani. Learning to recognize procedural activities with distant supervision. In *Proceedings of the IEEE/CVF Conference on Computer Vision and Pattern Recognition*, pages 13853–13863, 2022.
- [22] Zijia Lu and Ehsan Elhamifar. Set-supervised action learning in procedural task videos via pairwise order consistency. In Proceedings of the IEEE/CVF Conference on Computer Vision and Pattern Recognition, pages 19903–19913, 2022.
- [23] Pierre Simon Marquis de Laplace. Théorie analytique des probabilités, volume 7. Courcier, 1820.
- [24] Antoine Miech, Jean-Baptiste Alayrac, Lucas Smaira, Ivan Laptev, Josef Sivic, and Andrew Zisserman. End-to-end learning of visual representations from uncurated instructional videos. In *Proceedings of the IEEE/CVF conference on computer vision and pattern recognition*, pages 9879–9889, 2020.
- [25] Medhini Narasimhan, Licheng Yu, Sean Bell, Ning Zhang, and Trevor Darrell. Learning and verification of task structure in instructional videos. arXiv preprint arXiv:2303.13519, 2023.
- [26] Rohith Peddi, Shivvrat Arya, Bharath Challa, Likhitha Pallapothula, Akshay Vyas, Jikai Wang, Qifan Zhang, Vasundhara Komaragiri, Eric Ragan, Nicholas Ruozzi, et al. Captaincook4d: A dataset for understanding errors in procedural activities. arXiv preprint arXiv:2312.14556, 2023.
- [27] Chiara Plizzari, Gabriele Goletto, Antonino Furnari, Siddhant Bansal, Francesco Ragusa, Giovanni Maria Farinella, Dima Damen, and Tatiana Tommasi. An outlook into the future of egocentric vision. *International Journal fn Computer Vision*, 2023.
- [28] Shraman Pramanick, Yale Song, Sayan Nag, Kevin Qinghong Lin, Hardik Shah, Mike Zheng Shou, Rama Chellappa, and Pengchuan Zhang. Egovlpv2: Egocentric video-language pre-training with fusion in the backbone. In *Proceedings of the IEEE/CVF International Conference on Computer Vision*, pages 5285–5297, 2023.
- [29] Alec Radford, Jong Wook Kim, Chris Hallacy, Aditya Ramesh, Gabriel Goh, Sandhini Agarwal, Girish Sastry, Amanda Askell, Pamela Mishkin, Jack Clark, et al. Learning transferable visual models from natural language supervision. In *International conference on machine learning*, pages 8748–8763. PMLR, 2021.

- [30] Debaditya Roy, Ramanathan Rajendiran, and Basura Fernando. Interaction region visual transformer for egocentric action anticipation. In Proceedings of the IEEE/CVF Winter Conference on Applications of Computer Vision, pages 6740–6750, 2024.
- [31] Keisuke Sakaguchi, Chandra Bhagavatula, Ronan Le Bras, Niket Tandon, Peter Clark, and Yejin Choi. proScript: Partially ordered scripts generation. In Marie-Francine Moens, Xuanjing Huang, Lucia Specia, and Scott Wen-tau Yih, editors, Findings of the Association for Computational Linguistics: EMNLP 2021, pages 2138–2149, Punta Cana, Dominican Republic, November 2021. Association for Computational Linguistics.
- [32] Pol Schumacher, Mirjam Minor, Kirstin Walter, and Ralph Bergmann. Extraction of procedural knowledge from the web: A comparison of two workflow extraction approaches. In *Proceedings of the 21st International Conference on World Wide Web*, pages 739–747, 2012.
- [33] Fadime Sener, Dibyadip Chatterjee, Daniel Shelepov, Kun He, Dipika Singhania, Robert Wang, and Angela Yao. Assembly101: A large-scale multi-view video dataset for understanding procedural activities. In Proceedings of the IEEE/CVF Conference on Computer Vision and Pattern Recognition, pages 21096– 21106, 2022.
- [34] Steven S Skiena. The algorithm design manual, volume 2. Springer, 1998.
- [35] Sungryull Sohn, Hyunjae Woo, Jongwook Choi, and Honglak Lee. Meta reinforcement learning with autonomous inference of subtask dependencies. arXiv preprint arXiv:2001.00248, 2020.
- [36] Ashish Vaswani, Noam Shazeer, Niki Parmar, Jakob Uszkoreit, Llion Jones, Aidan N Gomez, Łukasz Kaiser, and Illia Polosukhin. Attention is all you need. Advances in neural information processing systems, 30, 2017.
- [37] Xin Wang, Taein Kwon, Mahdi Rad, Bowen Pan, Ishani Chakraborty, Sean Andrist, Dan Bohus, Ashley Feniello, Bugra Tekin, Felipe Vieira Frujeri, et al. Holoassist: an egocentric human interaction dataset for interactive ai assistants in the real world. In Proceedings of the IEEE/CVF International Conference on Computer Vision, pages 20270–20281, 2023.
- [38] Yoko Yamakata, Shinsuke Mori, and John A Carroll. English recipe flow graph corpus. In Proceedings of the Twelfth Language Resources and Evaluation Conference, pages 5187–5194, 2020.
- [39] Yiwu Zhong, Licheng Yu, Yang Bai, Shangwen Li, Xueting Yan, and Yin Li. Learning procedure-aware video representation from instructional videos and their narrations. In *Proceedings of the IEEE/CVF* Conference on Computer Vision and Pattern Recognition, pages 14825–14835, 2023.
- [40] Honglu Zhou, Roberto Martín-Martín, Mubbasir Kapadia, Silvio Savarese, and Juan Carlos Niebles. Procedure-aware pretraining for instructional video understanding. In *Proceedings of the IEEE/CVF Conference on Computer Vision and Pattern Recognition*, pages 10727–10738, 2023.
- [41] Luowei Zhou, Chenliang Xu, and Jason Corso. Towards automatic learning of procedures from web instructional videos. In *Proceedings of the AAAI Conference on Artificial Intelligence*, volume 32, 2018.
- [42] Yipin Zhou and Tamara L Berg. Temporal perception and prediction in ego-centric video. In *Proceedings of the IEEE International Conference on Computer Vision*, pages 4498–4506, 2015.
- [43] Dimitri Zhukov, Jean-Baptiste Alayrac, Ramazan Gokberk Cinbis, David Fouhey, Ivan Laptev, and Josef Sivic. Cross-task weakly supervised learning from instructional videos. In *Proceedings of the IEEE/CVF* Conference on Computer Vision and Pattern Recognition, pages 3537–3545, 2019.

A Evaluation Measures

This appendix details the evaluation measures used to assess performance experimentally for the two considered tasks of task graph generation and online mistake detection.

Task Graph Generation Task graph generation is evaluated by comparing a generated graph $\hat{G} = (\hat{\mathcal{K}}, \hat{\mathcal{A}})$ with a ground truth graph $G = (\mathcal{K}, \mathcal{A})$. Since task graphs aim to encode ordering constraints between pairs of nodes, we evaluate task graph generation as the problem of identifying valid pre-conditions (hence valid graph edges) among all possible ones. We hence adopt classic detection evaluation measures such as precision, recall, and F_1 score. In this context, we define True Positives (TP) as all edges included in both the predicted and ground truth graph (Eq. (7)), False Positives (FP) as all edges included in the predicted graph, but not in the ground truth graph (Eq. (8)), and False Negatives (FN) as all edges included in the ground truth graph, but not in the predicted one (Eq. (9)). Note that true negatives are not required to compute precision, recall and F_1 score.

$$TP = \hat{\mathcal{A}} \cap \mathcal{A}$$
 (7) $FP = \hat{\mathcal{A}} \setminus \mathcal{A}$ (8) $FN = \mathcal{A} \setminus \hat{\mathcal{A}}$ (9)

Online Mistake Detection We follow previous works on mistake detection from procedural egocentric videos [33, 37, 12] and evaluate online mistake detection with standard precision, recall, and F_1 scores. We break down metrics by the "correct" and "mistake" classes, as well as report average values.

B Implementation Details

This appendix provides implementation details to replicate the experiments discussed in Section 4.

B.1 Data Augmentation

In procedural tasks, it is common for certain actions to be repeated multiple times throughout the execution of a task. For example, in the EPIC-Tent dataset [17], an operation such as "reading the instructions" may be performed repeatedly at any point during the task. To model key-step orderings within the framework of topological sorts, our approach assumes that sequences should not contain such repetitions. Since repetitions denote that a specific action can appear at different stages of a procedure, we expand each sequence with repetitions to all distinct sequences obtained by dropping repeated actions. This data augmentation strategy enhances the robustness of our model on Assembly101 [33] and EPIC-Tent [17], while it was not necessary for the CaptainCook4D dataset [26], as sequences do not contain any repetitions.

B.2 Early Stopping

The learning process was conducted without the use of a validation set. To avoid overfitting and saving computation we defined a "Sequence Accuracy (SA)" score used to determine when the model reaches a learning plateau. We early stop models when an SA value of at least 0.95 is reached, and if the model shows no SA improvement for 25 consecutive epochs. The SA score is as follows:

$$SA = \frac{1}{|\mathcal{Y}|} \sum_{y \in \mathcal{Y}} \frac{1}{|y|} \sum_{i=0}^{|y|-1} c(y_i, y[:i], pred(y_i))$$
(10)

where \mathcal{Y} defined sequences in the training set, y is a sequence from \mathcal{Y} , y_i is the i-th element of sequence y, y[:i] are the predecessors of the i-th element in the sequence y, and $pred(y_i, Z)$ are the predicted predecessors for y_i from the current binarized adjacency matrix Z. The function c is defined as:

$$c(y_{i}, y[:i], pred(y_{i}, Z)) = \begin{cases} 1 & \text{if } |y[:i]| = 0 \text{ and } |pred(y_{i}, Z)| = 0\\ \frac{|y[:i] \cap pred(y_{i}, Z)|}{|pred(y_{i}, Z)|} & \text{if } |y[:i]| > 0 \text{ and } |pred(y_{i}, Z)| > 0\\ 0 & \text{otherwise} \end{cases}$$
(11)

The SA score measures the compatibility of each sequence with the current task graph based on the ratio of correctly predicted predecessors of the current symbol y_i of the sequence to the total number of predicted predecessors for y_i in the current task graph.

B.3 Hyperparameters

Table 4 details the hyperparameters employed in the experiments for task graph generation on the CaptainCook4D dataset [26]. During the training of TGT, we utilized a pre-trained EgoVLPv2 [28] to

Table 4: List of hyperparameters used in the models training process for task graph generation using CaptainCook4D [26].

	V	Value			
Hyperparameter	DO	TGT			
Learning Rate	0.1	0.000001			
Max Epochs	1000	1000			
Optimizer	Adam	Adam			
β^{-}	0.005	0.55			
Dropout Rate	-	0.1			

extract text and video embeddings. The temperature value T used in the cross-entropy distinctiveness loss was set to 0.9 as in [29].

For the downstream task of online mistake detection within the DO model framework, we extended the maximum training epochs to 1200 for Assembly101 [33]. This change was necessary because, even after 1000 epochs, the model continued to exhibit many cycles among its 86 nodes. Extending the number of epochs allows the model additional time to learn and minimize these cycles, which is crucial given the complexity of the graph. In the TGT configuration, we preserved the hyperparameters consistent with those used in the CaptainCook4D settings, except for adjusting the beta values to 1.

You are referred to the code for additional implementation details.

B.4 LLM Prompt

Below is the prompt that was employed to instruct the model on its task, which involves identifying pre-conditions for given procedural steps.

I would like you to learn to answer questions by telling me the steps that need to be performed before a given one.

The questions refer to procedural activities and these are of the following type:

 ${\tt Q}$ - Which of the following key steps is a pre-condition for the current key step "add brownie mix"?

- add oil
- add water
- break eggs
- mix all the contents
- mix eggs
- pour the mixture in the tray
- spray oil on the tray
- None of the above

Your task is to use your immense knowledge and your immense ability to tell me which preconditions are among those listed that must necessarily be carried out before the key step indicated in quotes in the question.

You have to give me the answers and a very brief explanation of why you chose them.

Provide the correct preconditions answer inside a JSON format like this:

```
{
   "add brownie mix": ["add oil", "add water", "break eggs"]
}
```

Table 5: A detailed breakdown of the data used from the CaptainCook4D dataset [26] for the task graph generation. This table categorizes each scenario by the number of videos, segments, and total duration in hours. The "Total" row aggregates the dataset characteristics.

Scenario	Videos	Segments	Duration
Microwave Egg Sandwich	5	60	0.9h
Dressed Up Meatballs	8	128	2.7h
Microwave Mug Pizza	6	84	1.2h
Ramen	11	165	2.7h
Coffee	9	144	2.2h
Breakfast Burritos	8	88	1.5h
Spiced Hot Chocolate	7	49	0.9h
Microwave French Toast	11	121	2.2h
Pinwheels	5	95	0.8h
Tomato Mozzarella Salad	13	117	1.3h
Butter Corn Cup	5	60	1.4h
Tomato Chutney	5	95	2.6h
Scrambled Eggs	6	138	2.6h
Cucumber Raita	12	132	2.7h
Zoodles	6	78	1.1h
Salted Mushrooms	7	126	2.9h
Blender Banana Pancakes	10	140	2.4h
Herb Omelet with Fried Tomatoes	8	120	2.4h
Broccoli Stir Fry	10	250	5.2h
Pan Fried Tofu	9	171	3.6h
Mug Cake	9	180	3.0h
Cheese Pimiento	7	77	1.6h
Spicy Tuna Avocado Wraps	9	153	2.6h
Caprese Bruschetta	8	88	2.4h
Total	194	2859	53.0h

B.5 Data Split

The CaptainCook4D dataset [26] comprises various error types, including order errors, timing errors, temperature errors, preparation errors, missing steps errors, measurement errors, and technique errors. Of these, missing steps and order errors directly impact the sequence integrity. Consequently, for our task graph generation, we utilized only those sequences of actions free from these specific types of errors. Table 5 shows statistics on the CaptainCook4D subsets used for task graph generation.

For Online Mistake Detection, we considered the datasets defined by the authors of PREGO [12].

In the context of pairwise ordering and forecasting, we employed the subset of the CaptainCook4D dataset designated for task graph generation (refer to Table 5) and divided it into training and testing sets. This division was carefully managed to ensure that 50% of the scenarios were equally represented in both the training and testing sets.

B.6 Pairwise ordering and future prediction

We setup the pairwise ordering and future prediction video understanding tasks following [42].

Pairwise Ordering Models take as input two randomly shuffled video clips and are tasked with recognizing the correct ordering between key-steps. We sample all consecutive triplets of labeled segments from test videos, discard the middle one, and consider the first and third ones as input pair. We evaluate models using accuracy.

Future Prediction Models take as input an anchor video clip and two randomly shuffled video clips and are tasked to select which of the two clips is the correct future of the anchor clip. We sample all consecutive triplets of labeled segments from test videos and consider the middle clip as the anchor and the remaining two clips as the two options. We evaluate models using accuracy.

Model We trained our TGT model using video embeddings extracted with a pre-trained EgoVLPv2 [28]. During the training process, if multiple video embeddings are associated with the same key-step across the training sequences, one embedding per key-step is randomly selected. The model is trained for graph generation on the training video and tested for pairwise ordering and future prediction on the test set. For pairwise ordering, we feed our model with the two clips and obtain a 2×2 adjacency matrix. We then select the ordering related to the largest off-diagonal weight. This weight denotes a $A \to B$ edge, suggesting a B, A order (B is a precondition of A). For future prediction, we feed the three clips and obtain a 3×3 adjacency matrix. We hence inspect the weights of edges $anchor \to A$ and $anchor \to B$ and choose as future clip, the one related to smallest weight (a small weights indicates that the selected clip is not a precondition).

Considered Data To evaluate the performance of high quality graph representations, for these experiments we consider the top-5 scenarios of CaptainCook4D, according to graph prediction performance obtained by our TGT model, namely: "Microwave Egg Sandwich", "Ramen", 'Tomato Mozzarella Salad", "Microwave French Toast", "Coffee".

B.7 Graph Post-processing

We binarize the adjacency matrix with the threshold $\frac{1}{n}$, where n is the number of nodes. After this thresholding phase, it is possible to encounter situations like the one illustrated in Figure 4, where node A depends on nodes B and C, and node B depends on node C. Due to the transitivity of the pre-conditions, we can remove the edge connecting node A to node C, as node B must precede node A. Sometimes, it may occur that a node does not serve as a pre-condition for any other node; in such cases, the END node should be directly connected to this node. Conversely, if a node has no pre-conditions, an edge is added from the current node to the START node.

At the end of the training process, obtaining a graph containing cycles is also possible. In such cases, all cycles within the graph are considered, and the edge with the lowest score within each cycle is removed. This method ensures that the graph remains a Directed Acyclic Graph (DAG).

B.8 Details on Online Mistake Detection

Given the noisy sequences in Assembly101 [33] and EPIC-Tent [17], a distinct approach was adopted during the post-processing phase of task graph generation. Specifically, if a key-step in the task graph has only two pre-conditions and one is the START node, the other pre-condition will be removed regardless of its score, otherwise we apply the transitivity dependences reduction aforementioned. This approach allows for a graph with fewer pre-conditions in the initial steps.

B.9 Qualitative Examples

Figure 5 reports a qualitative example of a prediction.

B.10 Experiments Compute Resources

The experiments involving the training of the DO model on symbolic data from the CaptainCook4D dataset proved to be highly efficient. We were able to generate all the task graphs in approximately half an hour using a Tesla V100S-PCI GPU. This GPU allowed us to run up to 8 training processes simultaneously. In contrast, training the TGT models for all scenarios in the CaptainCook4D dataset required about 24 hours, with the same GPU supporting the concurrent training of up to 2 models. Additionally, once the task graphs were obtained, executing the PREGO benchmarks for mistake detection was significantly faster, requiring online action prediction, which could be performed in real-time on a Tesla V100S-PCI GPU.

C Societal Impact

Reconstructing task graphs from procedural videos may enable the construction of agents able to assist users during the execution of the task. Learning task graphs from videos may be affected by geographical or cultural biases appearing in the data (e.g., specific ways of performing given tasks),

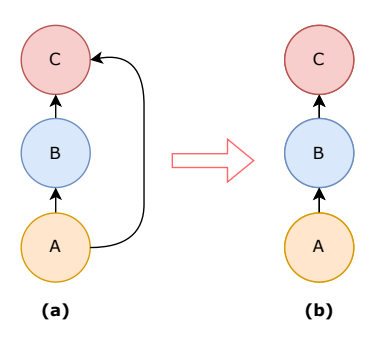


Figure 4: An example of transitive dependency between nodes. In (a) node A depends on B and C, but B depends on C, in this case, we can remove the edge between A and C for transitivity and we obtain the graph in (b).



Figure 5: A qualitative example of a graph predicted by our DO model on the "Microwave Egg Sandwich" scenario of CaptainCook4D [26]. Our method correctly predicts all ground truth edges (green ticks), but also tends to include some additional dependencies such as "top cup with salsa" \rightarrow "cut muffin" (red crosses), probably due to the dataset covering the most typical ways of performing the procedure.

which may limit the quality of the feedback returned to the user, potentially leading to harm. We expect that training data of sufficient quality should limit such risks.